

Conduction band structure of GaInP

P. Merle, D. Auvergne, and H. Mathieu

Centre d'Etudes d'Electronique des Solides,* Université des Sciences et Techniques du Languedoc, 34060-Montpellier-Cedex, France

J. Chevallier

Laboratoire du Centre National de la Recherche Scientifique, 92190-Meudon-Bellevue, France

(Received 26 January 1976)

The intrinsic absorption edge of $\text{Ga}_x\text{In}_{1-x}\text{P}$ alloys has been investigated by piezomodulation spectroscopy between helium and room temperature. The comparison of modulated reflectivity and transmission spectra gives clear evidence of the participation of L and X conduction minima to the indirect process. At 10°K , direct determination of the $\Gamma_{1c}-L_{1c}$ and $X_{1c}-L_{1c}$ crossover compositions ($x_c = 0.68$ and $x_c = 0.77$, respectively) permits one to resolve the discrepancies existing in the literature on this alloy. The contribution of resonant indirect transitions to $\Delta\epsilon_1$ is observed for the first time.

I. INTRODUCTION

During the last ten years a number of studies have been made on systems of mixed crystals of two III-V compounds. One interest in these works has been the synthesis of a semiconductor with a large direct energy gap for light-emitting-diode and laser applications, since all III-V compounds with an energy gap greater than 1.5 eV, have an indirect edge with the conduction-band minimum located near the X point of the Brillouin zone. It is well known¹ that a large-indirect-gap compound, alloyed with a smallest-direct-gap material will give a mixed crystal with a direct gap of intermediate magnitude. To obtain large-direct-gap devices with emitted radiation in the region of maximum eye sensitivity, systems such as $\text{GaAs}_{1-x}\text{P}_x$, $\text{Ga}_{1-x}\text{Al}_x\text{As}$, $\text{In}_{1-x}\text{Al}_x\text{P}$, and $\text{Ga}_x\text{In}_{1-x}\text{P}$ have been suggested.

From the point of view of band structure, $\text{In}_{1-x}\text{Al}_x\text{P}$ seems to be the optimal III-V material, as the highest direct band gap obtained (2.33 eV at 300°K).² From considerations of crystal growth, $\text{Ga}_x\text{In}_{1-x}\text{P}$ appears as one of the most suitable alloys for such applications. Recently, laser oscillations have been obtained on $\text{Ga}_x\text{In}_{1-x}\text{P}$ at energies up to 2.2 eV at 77°K ,³ illustrating the possibility to obtain light emission in the yellow-green part of the spectrum. Whatever the compound may be, it is very important for such applications to know the composition dependence of the energies of the conduction-band states since recombination from direct states (Γ_{1c}) are more efficient than from indirect ones (X_{1c} or L_{1c}).

In spite of the various works published on $\text{Ga}_x\text{In}_{1-x}\text{P}$ alloys, there is some controversy about the value of the composition at which the $\Gamma-X$ crossover of the conduction-band minima occurs. Using standard absorption,⁴ modulated spectro-

scopy (electroabsorption,⁵ thermoreflectance,⁶ and luminescence experiments)⁷ several authors found this $\Gamma-X$ crossover at $x = 0.64$ at room temperature, while cathodoluminescence^{8,9} and transport experiments³ give a rather higher value ($x = 0.74$). Until now, this large disagreement in the determination of the crossover composition has been attributed to material inhomogeneities or imperfections introduced by the different crystal preparations.⁵ In fact, all these experiments distinguished between direct and indirect edges without further precision about the identity of the indirect conduction-band minimum involved.

Recently, from high-pressure Hall-effect measurements on vapor epitaxial crystals of $\text{Ga}_x\text{In}_{1-x}\text{P}$ (with composition ranging between $x = 0$ and $x = 0.59$) Pitt *et al.*¹⁰ observed $\Gamma-L$ and $L-X$ electron transfers. Extrapolating their results for the entire system, they concluded that the $\Gamma-L$ and $L-X$ crossovers occur at compositions of the order of 0.63 and 0.74, respectively.

Largely due to the different values of the deformation potentials¹¹ of the L and X minima of zinc-blende compounds, it can be easily shown¹² that the strain-induced displacements of the $\Gamma_{1c}-\Gamma_{15v}$, $X_{1c}-\Gamma_{15v}$, $L_{1c}-\Gamma_{15v}$ transitions have well-defined phase relation allowing the direct identification of the conduction-band minimum involved in absorption process near indirect edge. It appears, then, that optical experiments on strained semiconductors would constitute the more-adequate procedure to obtain valuable information on long gap crossing.

We present here piezomodulation studies of the conduction-band structure of $\text{Ga}_x\text{In}_{1-x}\text{P}$ alloys. Comparing modulated reflectivity and transmission spectra, between 10 and 300°K we obtained direct evidence of the participation of the L and X minima to the absorption process occurring near the funda-

mental edge. On a sample of selected concentration we observed accurately direct-indirect crossover as a function of temperature.

II. EXPERIMENTAL TECHNIQUE

We have studied modulated optical absorption and reflection, in $\text{Ga}_x\text{In}_{1-x}\text{P}$ alloys obtained from a solution growth method. An indium bath is continuously fed by gallium from solid gallium phosphide and by phosphorus from vapor. The growth temperature is kept constant. Under these conditions, we obtain homogeneous polycrystalline ingots in the whole range of composition.¹³ Grain size is few square millimeters. Composition is determined by electron microprobe with a relative uncertainty of about 1% or 2%. For modulation spectroscopy experiments, samples are lapped and mechanically polished on one or two sides. The transmission and reflection spectra were taken between helium and room temperatures, using standard optical arrangement described elsewhere.¹² In order to obtain modulated spectra, $\text{Ga}_x\text{In}_{1-x}\text{P}$ samples are glued onto a piezoelectric transducer excited by a low-frequency alternating electric field.

III. THEORETICAL BACKGROUND

The lowest band edge in indirect zinc-blende-type semiconductors corresponds to transitions from the valence-band maximum at Γ to the lowest conduction-band minimum located at $k \neq 0$. In all the indirect binary compounds (AlP, AlAs, AlSb, GaP), this minimum is located at X point, but this is not always the case in pseudobinary alloys like $\text{Ga}_x\text{In}_{1-x}\text{P}$. This phenomenon is simply related to the sensitivity of the X point energy to the lattice constant, which is much smaller than that of the Γ and L points energies. So, studying the indirect edge of $\text{Ga}_x\text{In}_{1-x}\text{P}$ alloys, we must consider both the $\Gamma_{15v} - X_{1c}$ and the $\Gamma_{15v} - L_{1c}$ transitions.

Intermediate states and phonons involved in each of these processes are determined using the group theory formalism. They are illustrated in Fig. 1 where L_{1c} , Γ_{1c} , Γ_{15c} , X_{1c} , and L_{3v} , Γ_{15v} , X_{5v} are the irreducible representations of the electronic wave functions, and L_1 , L_3 , X_1 , X_3 , and X_5 represent the phonons symmetries which are in the case of GaP and InP:

$$X = X_5(\text{TO}) + X_5(\text{TA}) + X_1(\text{LA}) + X_3(\text{LO}),$$

$$L = L_3(\text{TO}) + L_3(\text{TA}) + L_1(\text{LA}) + L_1(\text{LO}).$$

For each scattering process (only one phonon involved), the absorption coefficient relative to indirect transitions from valence states to exciton states can be given by the general expression¹⁴

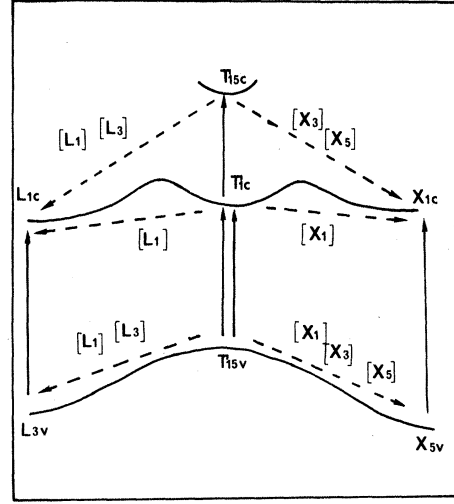


FIG. 1. Example of band-structure diagram for $\text{Ga}_x\text{In}_{1-x}\text{P}$ illustrating the different allowed phonon-scattering processes.

$$\alpha \sim \frac{P^2 H^2}{(\delta E \pm \hbar\omega_p)^2} (E - E_{g_x} \pm \hbar\omega_p)^{1/2}, \quad (1)$$

where P and H are, respectively, the matrix elements for radiative transition and phonon scattering, δE is the energy difference between the intermediate state and the final (or initial) state, and $\hbar\omega_p$ is the phonon energy.

Since the energy denominator of Eq. (1) is much smaller for the process involving the lowest conduction band Γ_{1c} , structures associated to this intermediate state will be expected to be the strongest. Now transitions via Γ_{1c} intermediate state involve only phonons of symmetries X_1 or L_1 (see Fig. 1). For $\Gamma_{15v} - X_{1c}$ indirect gap, LA(X) phonon-assisted transition is the strongest and for $\Gamma_{15v} - L_{1c}$ indirect gap, La(L) and LO(L) phonon-assisted transitions are the strongest.

When stress is applied to the solid, the initially fourfold-degenerate valence band is split into two doubly degenerate levels, and the equivalence of the various valleys of the conduction band is broken for certain stress directions. This gives a twofold modulation of the direct gap and a fourfold modulation of the indirect one, each component being polarization dependent. We have calculated¹² matrix elements and modulation amplitudes of these different transitions for different stress configurations, for all possible phonons, for all independent polarizations of light, and through all relevant intermediate states.

For (111) coplanar stress, used in these experiments, the different modulations of the threshold energy E_g , for the optical direct transitions Γ_{15v}

$\rightarrow \Gamma_{1c}$ and for the $\Gamma_{15v} \rightarrow X_{1c}$ and $\Gamma_{15v} \rightarrow L_{1c}$ indirect ones, are given, respectively, by

$$\frac{dE(\Gamma)}{dT} = 2 a_d (S_{11} + 2S_{12}) \pm \frac{d}{2\sqrt{3}} S_{44}, \quad (2a)$$

$$\frac{dE_x(X)}{dT} = 2 a_{ix} (S_{11} + 2S_{12}) \pm \frac{d}{2\sqrt{3}} S_{44}, \quad (2b)$$

$$\begin{aligned} \frac{dE_g(L)}{dT} = 2 a_{i1} (S_{11} + 2S_{12}) \\ + \theta(i, j, k) E_2^1 S_{44} \pm \frac{d}{2\sqrt{3}} S_{44}, \quad (2c) \end{aligned}$$

where the parameters S_{ij} are the compliance coefficients. a_d , a_{ix} , a_{i1} , E_2^1 , and d are the deformation potentials which specify the motion of the various transitions under the stress. $\theta(i, j, k) = -\frac{1}{3}$ for the $[111]$ valley and $\theta(i, j, k) = \frac{1}{6}$ for the $[\bar{1}11]$, $[1\bar{1}1]$, and $[11\bar{1}]$ valleys.

Thus, there is a twofold modulation of the $\Gamma_{15v} \rightarrow X_{1c}$ transition and a fourfold modulation of the $\Gamma_{15v} \rightarrow L_{1c}$ transition.

The effective piezomodulation strength of an absorption edge is calculated for all the modulated transitions, taking account for each process of the modulation amplitude, the matrix element, the effective masses of the electronic valence states and of the number of equivalent conduction band valleys. In particular, the piezomodulation parameter of the LA(X) phonon-assisted transition ($\Gamma_{15v} \rightarrow X_{1c}$ indirect gap) and that of the LA(L) and LO(L) phonon-assisted transitions ($\Gamma_{15v} \rightarrow L_{1c}$ indirect gap) are given, respectively, by¹²

$$\Delta[LA(X)] = \frac{1}{4} \frac{1}{1+\gamma} (2\alpha_x + \delta) + \frac{3}{4} \frac{\gamma}{1+\gamma} (2\alpha_x - \delta), \quad (3a)$$

$$\Delta[LA(L), LO(L)] = \frac{1}{4} \frac{1}{1+\gamma} (2\alpha_l + \delta) + \frac{3}{4} \frac{\gamma}{1+\gamma} (2\alpha_l - \delta), \quad (3b)$$

where $\alpha_x = a_{ix}(S_{11} + 2S_{12})$, $\alpha_l = a_{il}(S_{11} + 2S_{12})$, $\delta = d/(2\sqrt{3})S_{44}$, $\gamma = (m_1/m_2)^{3/2}$ take account of the different densities of the initial valence states, and the coefficients $\frac{1}{4}$ and $\frac{3}{4}$ determine the relative amplitudes of the matrix elements of the vertical transitions from the split Γ_{15v} valence band to the Γ_{1c} intermediate state.

Similarly the piezomodulation parameter of the direct transition $\Gamma_{15v} \rightarrow \Gamma_{1c}$ is given by

$$\Delta[E(\Gamma)] = \frac{1}{4} \frac{1}{1+\gamma} (2\alpha_d + \delta) + \frac{3}{4} \frac{\gamma}{1+\gamma} (2\alpha_d - \delta), \quad (3c)$$

where $\alpha_d = a_d(S_{11} + 2S_{12})$.

In the case of GaP, the elastic compliance constants S_{ij} (in units of 10^{-6} bar⁻¹), the deformation potential (in eV) and the γ coefficient are, respectively,¹⁵

$$S_{11} = 1.05, \quad S_{12} = -0.34, \quad S_{44} = 1.55;$$

and¹⁵⁻¹⁸

$$a_d = 9.29, \quad a_{ix} = -3.7, \quad a_{il} = 2.48,$$

$$d = -4, \quad \gamma = 8.$$

This gives

$$\Delta[E(\Gamma)] = 5.9 \times 10^{-6} \text{ eV/bar},$$

$$\Delta[LA(X)] = -0.8 \times 10^{-6} \text{ eV/bar},$$

$$\Delta[LA(L), LO(L)] = 2.42 \times 10^{-6} \text{ eV/bar}.$$

The most-significant result here is that $\Delta[LA(X)]$ is small and negative, whereas $\Delta[E(\Gamma)]$ and $\Delta[LA(L)]$ or $[LO(L)]$ are larger and positive. It is important to verify that at least the relative sign is independent of uncertainties in the determination of various deformation potentials. The largest uncertainties concern a_{il} which is not determined experimentally. In order to compare these signs, it is possible to simplify Eqs. (3) on account of the order of magnitude of the different coefficients (particularly $3\gamma \gg 1$). We obtain

$$\frac{\Delta[LA(X)]}{\Delta[LA(L), LO(L)]} \approx \frac{2\alpha_x - \delta}{2\alpha_l - \delta}. \quad (4)$$

Considering first the numerator, we note that, α_x and δ being experimentally measured on GaP, we can consider as established the negative sign of this term.

Focusing now on the denominator, we note that δ is negative (different measurements^{15,17}) and α is always positive (calculated value¹⁶ on GaP and experimental value¹⁶ on Ge). So that the positive sign of this term can also be considered as established, the α_l value is not measured in GaP.

In essence, the important result is that the $\Gamma_{15v} \rightarrow L_{1c}$ indirect transition, involving both the LA(L) and the LO(L) phonons, and the $\Gamma_{15v} \rightarrow \Gamma_{1c}$ direct transition are piezomodulated with the same phase, while the $\Gamma_{15v} \rightarrow X_{1c}$ indirect transition involving the LA(X) phonon is piezomodulated in opposite phase. Consequently, it will be possible in piezotransmission measurement to distinguish $\Gamma_{15v} \rightarrow X_{1c}$ from $\Gamma_{15v} \rightarrow L_{1c}$ indirect gap.

It is important to note that these results, obtained on single crystal can be extended to polycrystals.

In a polycrystal it is possible to define a new medium, isotropic by compensation, characterized by average compliance constants \bar{S}_{ij} given in cubic materials by¹⁶

$$\begin{aligned} \bar{S}_{11} &= \frac{3}{5} S_{11} + \frac{2}{5} S_{12} + \frac{1}{5} S_{44}, \\ \bar{S}_{12} &= \frac{1}{5} S_{11} + \frac{4}{5} S_{12} - \frac{1}{10} S_{44}, \\ \bar{S}_{44} &= \frac{4}{5} S_{11} - \frac{4}{5} S_{12} + \frac{3}{5} S_{44}. \end{aligned} \quad (5)$$

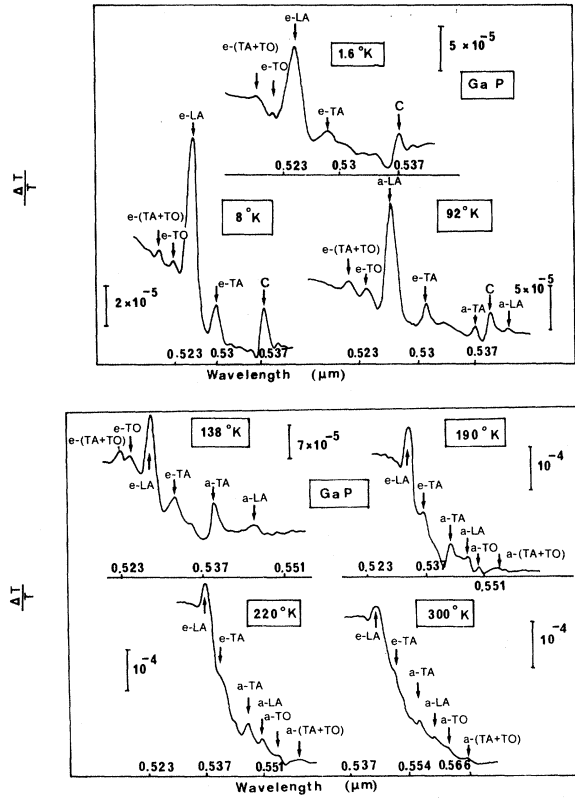


FIG. 2. Piezotransmission spectra near the fundamental edge of $\text{Ga}_x\text{In}_{1-x}\text{P}$ crystals, for values of the composition $x = 1, 0.915,$ and $0.84,$ respectively. Recorded spectra are given at different temperatures between helium and room temperatures. The temperature evolution of these spectra shows clearly the influence of the background contribution produced by the nonresonant indirect processes. The different phonon processes are indicated relative to the phonon branch involved; the subscripts denote whether the phonon is emitted (e) or absorbed (a).

Under arbitrary coplanar stress [(111) for illustration], $\bar{\alpha}$ and $\bar{\delta}$ parameters are given by

$$\bar{\alpha} = \bar{a}_i(\bar{S}_{11} + 2\bar{S}_{12}), \quad (6)$$

$$\bar{\delta} = (\bar{d}/2\sqrt{3})\bar{S}_{44}. \quad (7)$$

\bar{d} is a shear-deformation potential, so that $\bar{d} = 0$. On the other hand, a_i , which is the hydrostatic component, gives $\bar{a}_i = a_i$. The result is

$$\bar{\alpha} = \alpha \text{ and } \bar{\delta} = 0,$$

so that

$$\frac{\Delta[\text{LA}(X)]}{\Delta[\text{LA}(L), \text{LO}(L)]} \approx \frac{\bar{\alpha}_x}{\bar{a}_i} = \frac{a_{ix}}{a_{ii}}. \quad (8)$$

This ratio is negative because in all the materials a_{ix} is negative and a_{ii} is positive.

IV. RESULTS AND DISCUSSION

A. $\Gamma_{15v} - X_{1c}$ transitions

Figures 2–4 give some representative piezotransmission spectra for $\text{Ga}_x\text{In}_{1-x}\text{P}$ samples, in the temperature range 1.6–300°K, corresponding to the values $x = 1, 0.915,$ and $0.84.$ The piezotransmission spectra of GaP have been discussed in a preceding paper²⁰ and are given here for comparison in order to interpret the structures observed on the pseudobinary system. For samples of low-indium content it is expected that the lowest band edge corresponds to indirect transitions from the valence-band maximum Γ_{15v} to the lowest-conduction-band minimum X_{1c} . Phonons involved in the scattering process are identified from symmetry considerations.^{21,22} The main structures observed on²⁰ Gap [Fig. 2(a)] at helium temperature corresponds to the excitonic indirect process assisted by the emission of LA phonon, via the Γ_{1c} intermediate state. The weaker structures on the low-energy side correspond, respectively, to the TA process (via X_{5v} or Γ_{15c}) and to impurity transition.

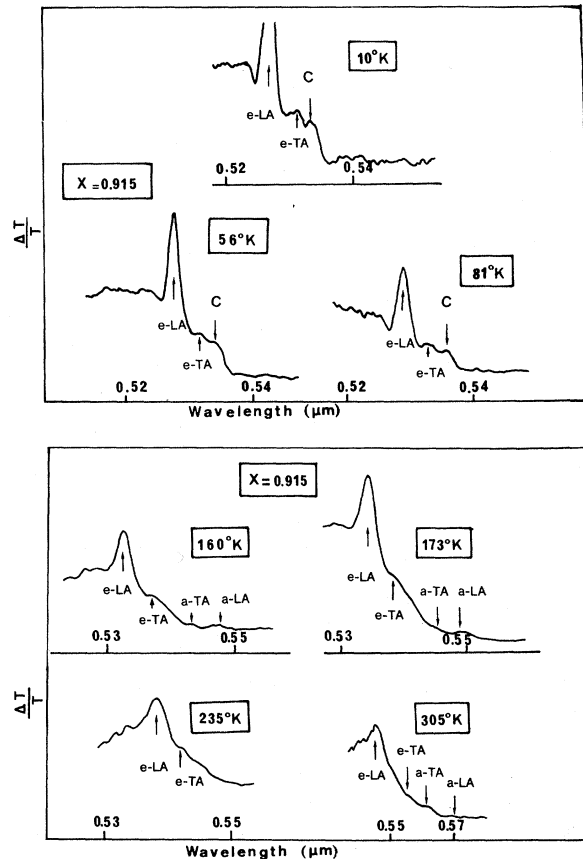


FIG. 3. Same as Fig. 2.

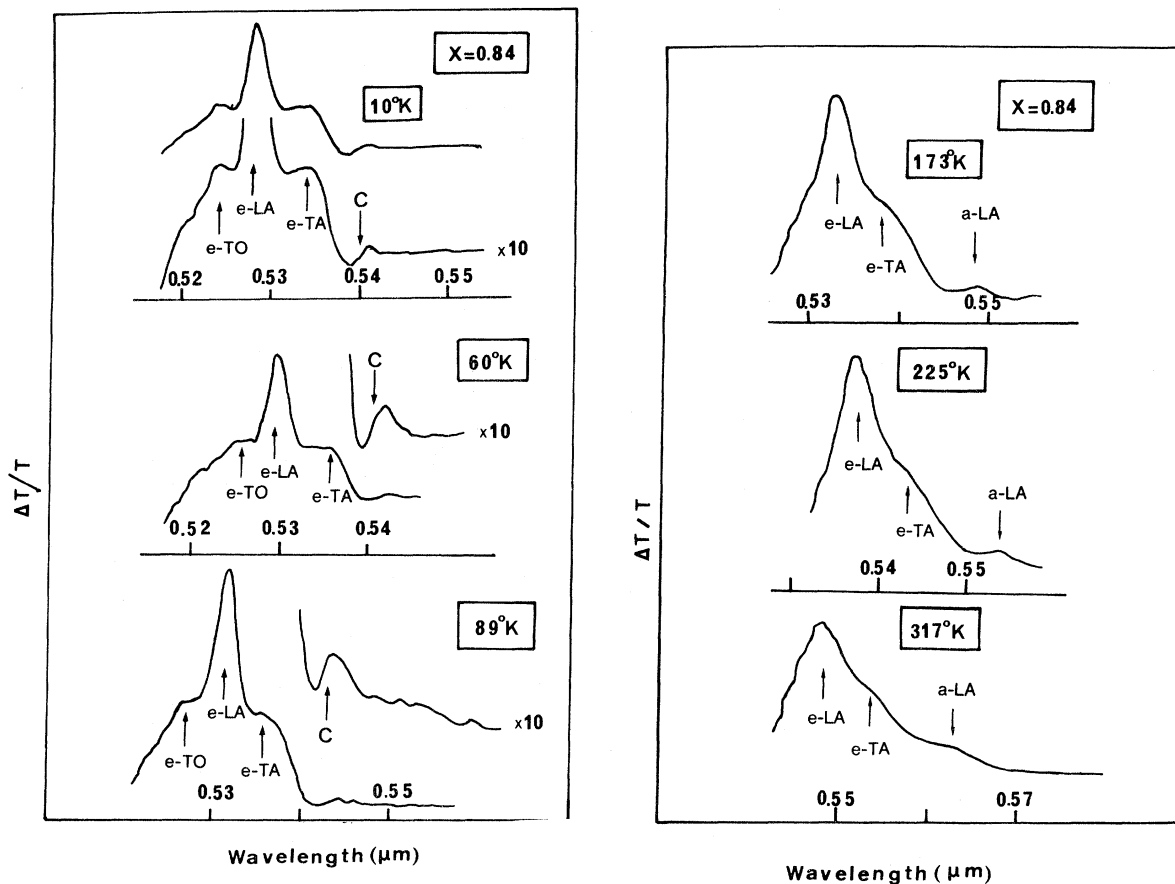


FIG. 4. Same as Fig. 2.

The piezotransmission spectra obtained on $x = 0.915$ and $x = 0.84$ samples (Figs. 3 and 4) show structures similar to those observed for the pure GaP compound. The relative phases of these spectra are the same. This implies the participation of X_{1c} conduction minima in the indirect process (see discussion in Sec. III). The main structure corresponding to LA-phonon scattering is as well resolved as that for GaP.

The structures C at 2.309, 2.325, and 2.300 eV observed on the low-temperature spectra (for $x = 1, 0.915,$ and 0.84 , respectively) present a strong excitonic character. Well resolved at low temperature, they disappear completely above 100°K . This zero-phonon transition can certainly be attributed to an exciton bound to a residual impurity whose definite identification cannot be obtained without complementary luminescence studies on specially doped samples.²³

The definite identification of the different structures is obtained from their temperature evolution. The increase of phonon density at a temperature higher than nitrogen temperature permits one to observe the complete pair-component spectra.

As the temperature increases, the phonon occupation number becomes comparable to unity and the process involving absorption of phonons becomes appreciable. The corresponding components are clearly shown on the high-temperature spectra in Figs. 2(b), 3(b), and 4(b). The identification of the different structures is correlated to their temperature dependence. The most important new structures correspond to the absorption of TA and LA phonons; note the broadening of the high-temperature spectra, due to the increase of the phonon-absorption components. The temperature evolution of the energy of the different structures is shown in Figs. 5–7, with their identification. For each structure, the small dispersion of the experimental points permits a good determination of the energy of the different phonons and of the temperature coefficient of the threshold.

Let $\hbar\omega_{a(e)}(\text{LA})$ denote the threshold energy for indirect transition assisted by absorption (emission) of LA phonons at X , and similarly for TO and TA phonons. Between 80 and 300°K the quantities $\frac{1}{2}[\hbar\omega_a(\text{LA, TA}) + \hbar\omega_e(\text{LA, TA})]$ give for the excitonic energy gap E_{gx} two values consistent to

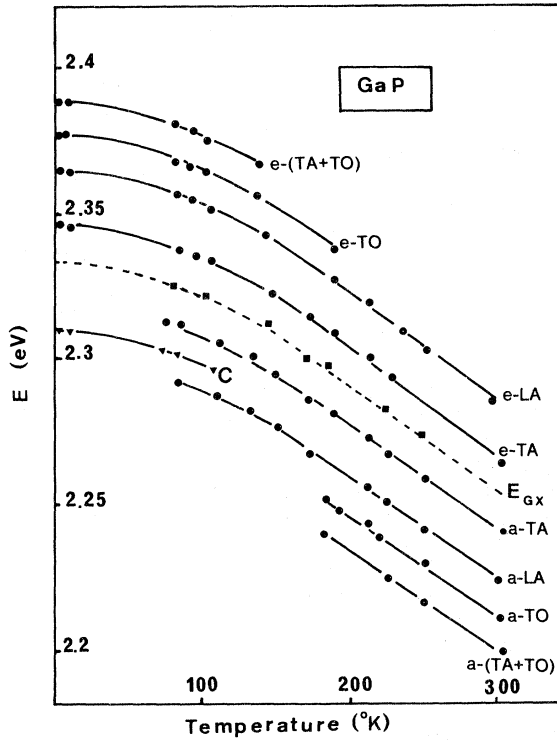


FIG. 5. Temperature dependence of the thresholds of the absorption components indicated in Figs. 2-4. The solid circle, solid square, and triangle points correspond to the experimental points; solid squares represent the only nonexcitonic process clearly resolved (Ref. 21), and solid triangles to exciton impurity complexes.

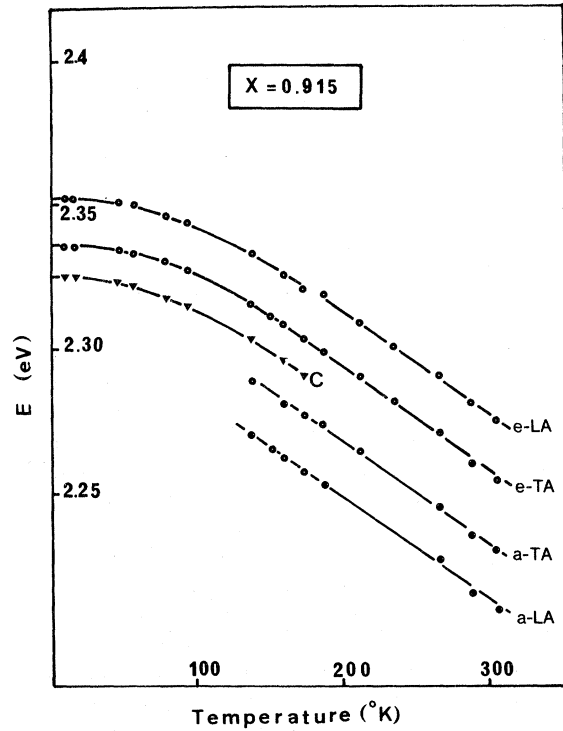


FIG. 6. Same as Fig. 5.

better than 0.1%. This gives the temperature variation of E_{gx} represented by a dashed line in Figs. 5-7. Conserving equal spacing between this line and the e -TA and e -LA lines, gives extrapolated value of 2.333, 2.321, and 2.315 eV for the indirect exciton gap corresponding, respectively, to $x=1$, 0.915, and 0.84 samples at helium temperatures. Between 160 and 300 °K, E_{gx} decreases linearly with a slope of $3.7 \cdot 10^{-4}$ eV/°K nearly constant from $x=1$ to $x=0.84$. As already mentioned, this constant value of dE_{gx}/dT reflects the relative insensitivity of x minima to the variation of lattice constant, and the fact that the form factors which may be used to describe the energy gaps have nearly constant values along the investigated composition range.^{24,25}

The phonon-energy values are accurately obtained from the energy difference $\frac{1}{2}(\hbar\omega_e - \hbar\omega_a)$ corresponding to the pair components of Figs. 5-7. The values we deduced (listed in Table I) are shown in Fig. 8. Extrapolating the TA and LA energies from InP,²⁶ we verify that the energy of the phonons belonging to the acoustical branch as-

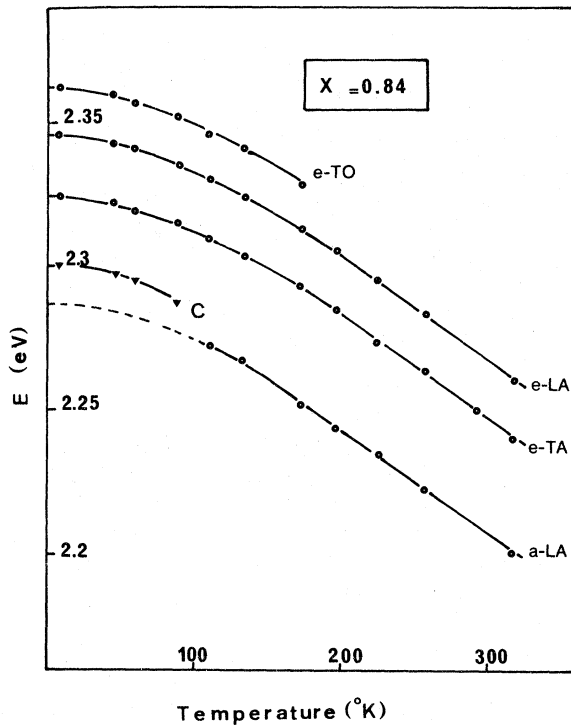


FIG. 7. Same as Fig. 5.

TABLE I. Comparison of phonon energies at X obtained on $\text{Ga}_x\text{In}_{1-x}\text{P}$ samples (a) in this work; (b) from Ref. 32.

Composition x	Experimental phonon energies (meV)		
	LA	TA	TO
1 ^a	32 ± 1	13 ± 1	44
0.915 ^a	31 ± 2	13 ± 2	
0.84 ^a	30 ± 2	11 ± 2	
0 ^b	15.5	8.3	35

sumes a nearly linear variation with composition. This result is in agreement with the conclusions of the modified random-element displacement²⁷ which predicts one-mode behavior for $\text{Ga}_x\text{In}_{1-x}\text{P}$. This behavior has been found by Lucovsky *et al.*²⁸ and more recently by Beserman *et al.*²⁸ in studying long-wavelength optical phonons by infrared and Raman spectroscopy.

Note, however, that the good definition of the phonon structure we observed is comparable to that of the pure compound. We have not observed disorder effects as was observed by Onton *et al.*²⁹ on $\text{Ga}_x\text{As}_{1-x}\text{P}$ (creation of zero-phonon free exciton by disorder scattering) or by Lucovsky *et al.*³⁰ on $\text{Ga}_x\text{In}_{1-x}\text{P}$ (disorder-induced process involving zone-boundary phonons to explain fine structures in the reststrahlen band).

B. Phase relation between direct and indirect transitions

As mentioned in Sec. III, the well-defined phase relation which exists in the modulation of direct and indirect edges must permit the identification of the zone boundary involved. In order to obtain unambiguous information, it is necessary to observe simultaneously on the same spectrum, structure characteristic of direct and indirect transitions. For that, we measured (Figs. 9 and 10) $\Delta R/R$ spectra on thin samples with the front and the back faces optically polished. The reflec-

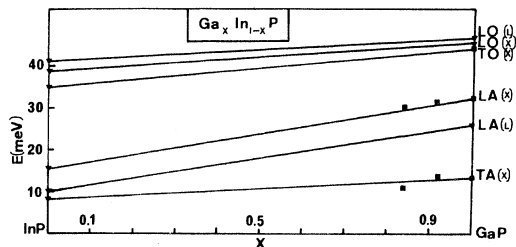


FIG. 8. Composition dependence of phonon energy values deduced from piezotransmission spectra: ■, experimental points; ▼, Ref. 32.

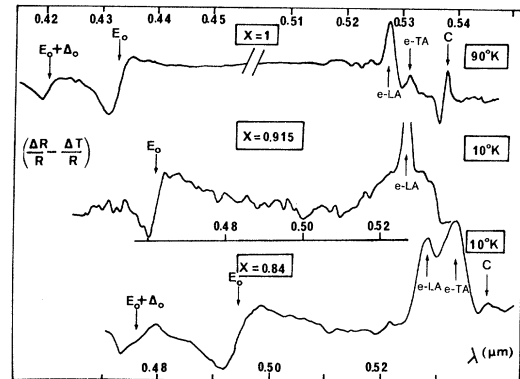


FIG. 9. Piezorefectivity spectra obtained on $\text{Ga}_x\text{In}_{1-x}\text{P}$ samples, with two faces optically polished. The reflected beam, on the front face, gives the high-energy structures characteristic of direct transitions ($\Delta R/R$ part); structures characteristic of indirect transitions are contained in the beam reflected from the back face ($-\Delta T/R$ part). As discussed in the text, for each composition, the relative phase of the spectra permits to identify the conduction minima involved in the indirect process.

tion on the front face gives

$$\Delta R/R = \alpha \Delta \epsilon_1 + \beta \Delta \epsilon_2. \quad (9)$$

At an energy near that of the direct edge, $\beta \Delta \epsilon_2$ is smaller than³¹ $\alpha \Delta \epsilon_1$ and may be neglected (these two terms are comparable only at energies corresponding to E_1 transitions). So the front face gives $\Delta R/R = \alpha \Delta \epsilon_1$, i.e., only direct transitions

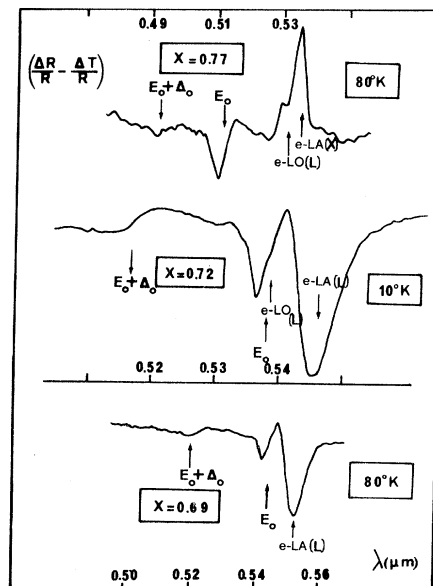


FIG. 10. Same as Fig. 9.

are important in these spectra since there is no contribution of indirect transitions to $\Delta\epsilon_1$.

The reflection on the back face, adds a supplementary term proportional to ΔT ie to $\Delta\epsilon_2$.³² In this case expression (9) becomes

$$\Delta R/R = \alpha \Delta\epsilon_1 - \beta' \Delta\epsilon_2, \quad (10)$$

where $\beta' \Delta\epsilon_2 \sim \Delta T$ may contain all structures in the density of states like indirect edges occurring at energies lower than that of the direct edge. We must note that near the E_0 direct edge, due to the high values of the absorption coefficient, this term vanishes completely. Finally, this gives

$$\frac{\Delta R}{R} \sim \frac{d\epsilon_1}{dE} \Delta E_{\text{direct}} - \frac{d\epsilon_2}{dE} \Delta E_{\text{indirect}}. \quad (11)$$

The study of these structures has two aims: (i) to observe simultaneously structures corresponding to direct and indirect edges, in order to obtain more accurate information about their crossover, and (ii) to specify the identity of the zone boundary involved in the indirect process, from the relative phases of the modulation amplitudes.

Figure 9 gives a clear illustration of the differential-reflectivity spectra [Eq. (11)] that we have observed on $\text{Ga}_x\text{In}_{1-x}\text{P}$ samples ($x=1, 0.915,$ and 0.84). The structures corresponding to the direct edge are excitonic and have the shape of a two-dimensional minimum of the density of states³³ [Fig. 11(a)]; those corresponding to the clearly resolved indirect edges, are lightly modified compared to those of Figs. 2–4, because here we obtained $\Delta T/R$ and not $\Delta T/T$. Note the decrease of the energy separation with composition between the structures as x decreases. These spectra constitute the first clear visualization of direct- and indirect-gap crossover.

The relative phase of the structures is discussed in agreement with the line shapes shown in Fig. 11, Figures 11(a) and 11(b) represent the line shape of the modulated dielectric constant we may expect to observe for direct and indirect excitonic gaps.³³ In agreement with Eq. (11), to reproduce the spectra of Fig. 9 we must combine $\Delta\epsilon_1$ of Fig. 11(a) with $\Delta\epsilon_2$ of Fig. 11(b). If the direct and indirect gaps are modulated with the same phase, the $\Delta R/R$ spectrum must be identical to that of Fig. 11(c). On GaP and $\text{Ga}_x\text{In}_{1-x}\text{P}$, for $x=0.915$ and 0.84 (Fig. 9), the relative phase of the structures is the opposite of this case. On the other hand the line shape in Fig. 9 is similar to that shown in Fig. 11(d). This, shows without ambiguity that the direct gap E_0 and the indirect one, are modulated out of phase. As argued in the piezomodulation calculation of Sec. III, this demonstrates that the indirect transition observed in Fig. 9, involves X minima of the conduction band.

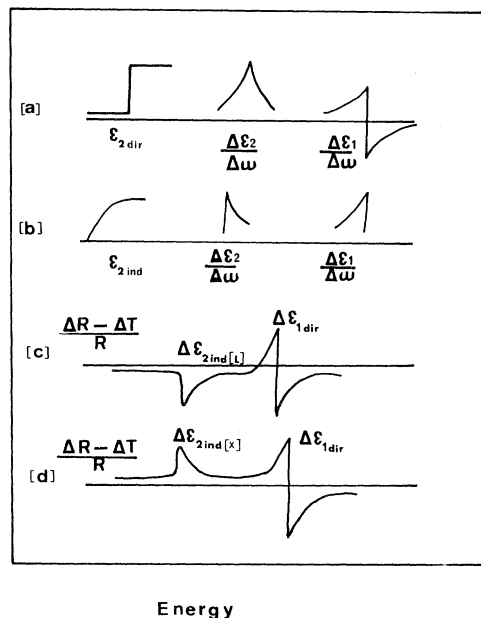


FIG. 11. Illustration of the different line shapes expected from the mixture of reflection and transmission spectra. Insets (a) and (b) give the theoretical line shapes of $\Delta\epsilon_1$ and $\Delta\epsilon_2$ for direct and indirect excitonic edges; insets (c) and (d) give the $(\Delta R - \Delta T)/R$ line shapes corresponding to direct and indirect transitions ending at L and X minima, respectively.

L minima would produce the line shape of Fig. 11(c).

In Fig. 10 we give identical spectra to those previously observed, but obtained on $x=0.77, 0.72,$ and 0.69 , $\text{Ga}_x\text{In}_{1-x}\text{P}$ samples. For $x=0.77$, the direct and indirect gaps are less than 100 meV from each other; the relative phase of the structures shows, as in the preceding discussion, that the indirect process occurs at X minima.

For $x=0.72$ and $x=0.69$ there is a drastic change in the line shape. The relative phase of the individual structures is reversed and this shows [Fig. 11(c)] that the direct and indirect gaps are modulated in phase. This new structure is not associated with an impurity for the following reasons. This structure is very close to Γ and X conduction-band minima, so if an impurity level is involved this is associated with Γ or X minima. The structure observed is in phase with the one due to the E_0 gap, and in opposite phase with the one due to the E_{ind}^x gap; so if this is an impurity structure, the impurity level is associated with the Γ minimum. Now Figs. 15, 16, 19, and 20 show that the temperature coefficient of the structure is different than that of

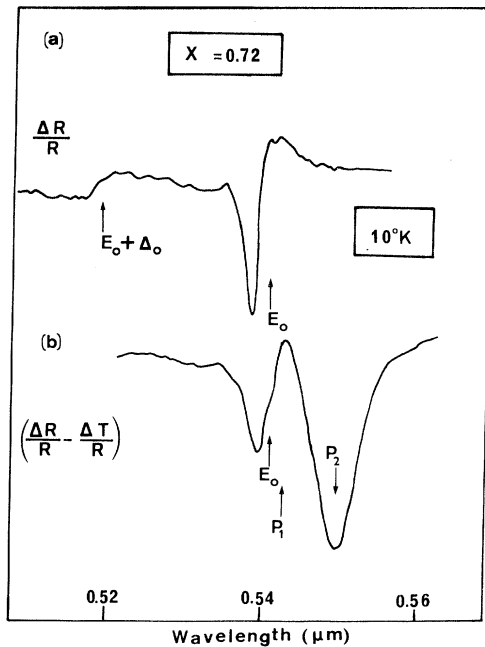


FIG. 12. Illustration of the back-reflection contribution to the $\Delta R/R$ spectra, obtained on $x = 0.72$ sample. Curve (a) is obtained on sample with a rough back face and curve (b) on the same sample with the two faces optically polished. These spectra give also clear evidence of the proximity of $\Gamma-L$ crossover.

the E_0 gap. Another reason is that Fig. 14 shows the existence of two structures whose energy difference is in agreement with the energy difference between the two phonons $LO(L)$ and $LA(L)$, which are precisely the allowed phonon structures for an L indirect gap.

This result constitutes the first clear evidence for this alloy of the participation of L minima in the indirect process. Although these spectra which show $(\Delta R - \Delta T)/R$ are very useful for comparing the relative phases of the structures due to direct and indirect transitions, they do not allow an accurate determination of the various structures. This limitation is due to large reduction of $\Delta T/R$ by the absorption in the sample. Thus, for accurate determination of the various band gaps we use piezotransmission $\Delta T/T$ and piezoreflection spectra $\Delta R/R$. This is discussed next.

C. $\Gamma-L$ crossover

Figure 12 gives the comparison of the $\Delta R/R$ spectra obtained on the $x = 0.72$ sample in the two following cases: (a) sample with a rough back face and (b) sample with optically polished back face. Curve (a) corresponds to $\Delta R/R \sim \Delta\epsilon_1$, the struc-

ture observed is characteristic of E_0 excitonic and $E_0 + \Delta_0$ transitions and is similar to the spectra we have given in Fig. 9 (high-energy part of the spectra). Curve (b) contains two more structures P_1 and P_2 induced by ΔT . These structures in phase with that of E_0 , are out of phase with respect to the structures characteristic of the indirect gap at X (see Fig. 9).

In agreement with the piezomodulation calculation of direct and indirect gaps (Sec. III and Fig. 11), this phase inversion permits us to assign these structures to transitions ending at the L_{1c} minimum of the conduction band. In the Fig. 13, we compare the $(\Delta R - \Delta T)/R$ and $\Delta T/T$ spectra observed at $10^\circ K$ on the sample with two optically polished faces. In transmission spectra, the P_1 and P_2 structures are clearly resolved. They are attributed to the $\Gamma_{15v} - L_{1c}$ transitions, assisted by the scattering of $LO(L)$ and $LA(L)$ phonons, which are the only scattering processes allowed by Γ_{1c} . The energy difference between these two structures (22 meV), obtained from Fig. 14, is in good

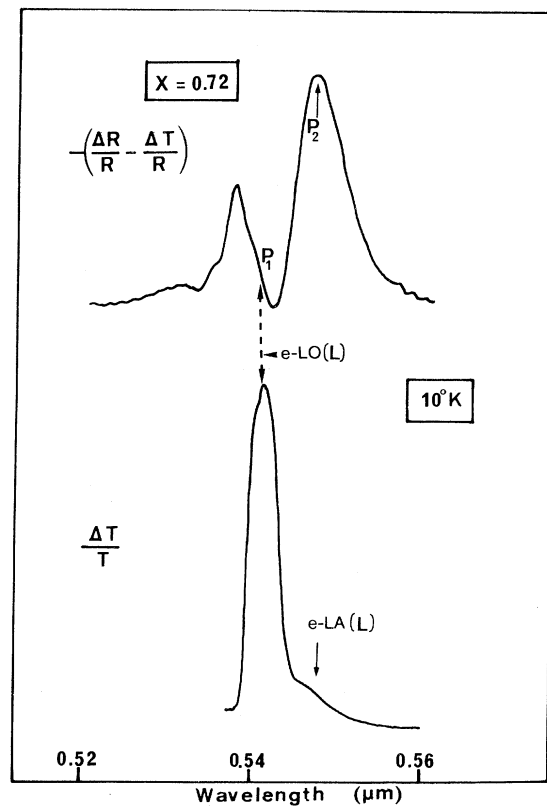


FIG. 13. Comparison of $(\Delta R - \Delta T)/R$ and $\Delta T/T$ spectra. The transmission spectrum shows clearly the two scattering processes involved in the indirect transition.

TABLE II. Comparison of the values of the direct (E_0, E_1) and indirect transitions with their temperature coefficients obtained in this work. Δ_0 spin-orbit splitting values are also given for completeness.

Composition x	E_0 (eV) 300 °K	E_0 (eV) 80 °K	$\frac{dE_0}{dT}$ (10^{-4} eV/°K)	Δ_0 (meV)	E_1 (eV) 300 °K	$\frac{dE_1}{dT}$ (10^{-4} eV/°K)	Impurity (eV) 10 °K	$E_{\text{ind}} - E_{\text{ex}} + \hbar\omega_{\text{LA}}(x)$ (eV) 10 °K	$E_{\text{ind}} - E_{\text{ex}} + \hbar\omega_{\text{LO(L)}}$ (eV) 10 °K	
1	2.773	2.864	-5.1	81	3.706	-4.1	2.309	2.364		
0.915	2.587	2.678	-4.8	83-86			2.325	2.352		
0.84	2.422	2.505	-4.95	95	3.516	-4.3	2.300	2.345		
0.77	2.328	2.418	-4.8	95	3.465	-4.2			2.329	
0.72		2.289	-4.8	104					2.297	
										$dE/dT = -4.4 \times 10^{-4}$ eV/°K
0.69										2.270

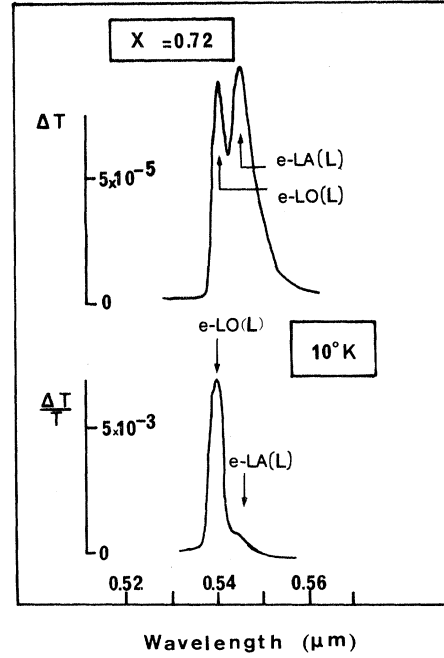


FIG. 14. Comparison of $\Delta T/T$ and ΔT spectra. The screening of ΔT structures by the $(-2\alpha d)$ term, allows an accurate determination of the energy difference between the LO and LA structures.

agreement with the difference $\hbar\omega_{\text{LO(L)}} - \hbar\omega_{\text{LA(L)}} = 23.5$ meV deduced from the linear extrapolation of the phonon energies of the pure compounds.²⁷ At 10 °K, we obtain for the energy of the direct and indirect gaps the values

$$E_0 = 2.303 \text{ eV [from Fig. 12(a)],}$$

$$\left. \begin{aligned} E_{\text{ind}} - E_{\text{ex}} + \hbar\omega_{\text{LO(L)}} &= 2.297 \text{ eV} \\ E_{\text{ind}} - E_{\text{ex}} + \hbar\omega_{\text{LA(L)}} &= 2.275 \text{ eV} \end{aligned} \right\} \text{(from Fig. 14).}$$

Taking account of the temperature coefficients of E_0 and E_1 transitions (Ref. 34 and Table II, where we show that dE_0/dT is greater than dE_1/dT) and of the vicinity of the transitions at 10 °K, we may expect to observe at higher temperature the crossing of the E_0 and $E_{\text{ind}} - E_{\text{ex}} + \hbar\omega_{\text{LO(L)}}$ transitions, that is the resonance of the indirect transition assisted by emission of LO phonon.

This resonance which corresponds to the vanishing of the denominator of Eq. (1), has until now, never been observed, and is clearly shown in Figs. 15-17. Figures 15 and 16 show the temperature evolution of the $\Delta R/R$ structures corresponding to the E_0 gap, observed on the sample with unpolished back face. At low temperature, we observe a structure characteristic of excitonic direct gap transition. At higher temperature (greater than 100 °K) an extra oscillation appears

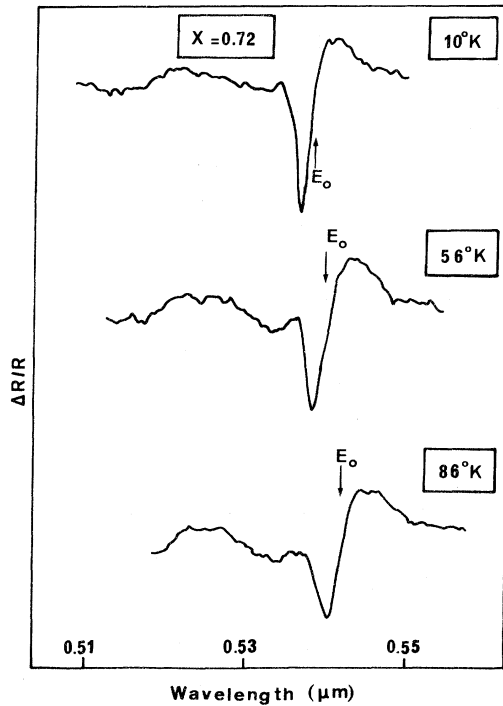


FIG. 15. Temperature evolution of $\Delta R/R$ spectra obtained on $\text{Ga}_{0.72}\text{In}_{0.28}\text{P}$ sample, with rough back face. The extra oscillation appearing at temperature greater than 135°K gives clear evidence of the contributions to $\Delta\epsilon_1$ of resonant indirect transitions.

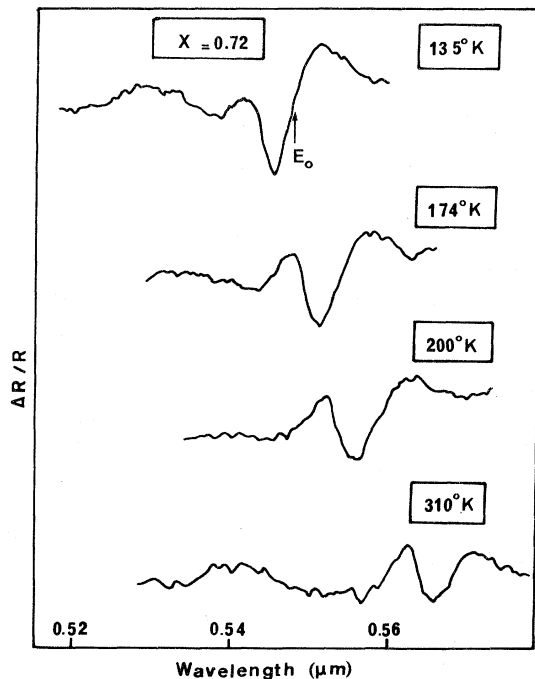


FIG. 16. Same as Fig. 15.

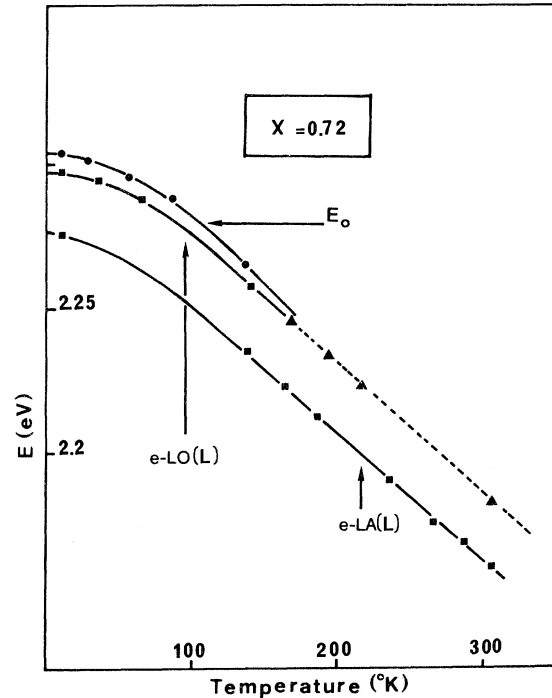


FIG. 17. Temperature dependence of the thresholds of the direct and indirect edges observed on $\text{Ga}_{0.72}\text{In}_{0.28}\text{P}$ sample. Solid circles represent the energy of direct edge deduced from $\Delta R/R$ spectra [Fig. 12(a)], solid squares correspond to the energies of the absorption components indicated in Fig. 14, solid triangles represent the energy of the structures obtained on $\Delta T/T$ spectra, produced by the mixing of E_0 and $\text{LO}(L)$ structures. The temperature evolution of these energies gives direct evidence of the Γ - L crossover.

(Fig. 16). We have plotted in Fig. 17 the temperature evolution of the energies of the direct (Fig. 15) and indirect transitions ($E_{\text{ind}} - E_{\text{ex}} + \hbar\omega_{\text{LO}(L)}$ and $E_{\text{ind}} - E_{\text{ex}} + \hbar\omega_{\text{LA}(L)}$) of Figs. 13 and 14, it shows that the crossover appears at temperatures greater than 135°K .

These extra oscillations correspond to a resonance of the indirect transition produced by the achievement of energy conservation with the intermediate state which becomes the resonant state. [This can be seen from expression (1) for the imaginary part of the dielectric constant.] This means that the contribution to ϵ_1 of the indirect transition can become comparable to that of a direct gap. This explains the modification of the $\Delta R/R$ structures at temperatures above the value at which direct and indirect edges are very close (this is shown by the comparison of the low- and high-temperature spectra of Figs. 15 and 16).

In a first approximation we can test this result, comparing on the absorption curve of GaP obtained

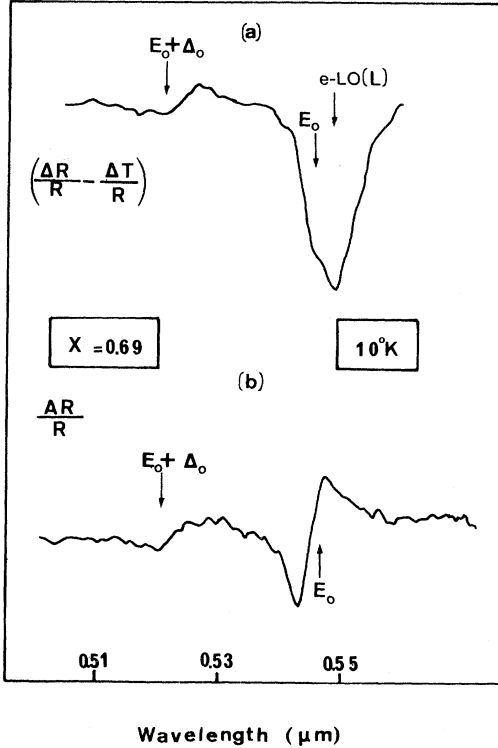


FIG. 18. Illustration of the proximity of the Γ - L crossover on reflectivity spectra obtained on $x = 0.69$ sample with (a) two faces optically polished and (b) the same sample with a rough back face.

by Dean *et al.*,³⁵ the value of ϵ_2 at the energy of the direct gap, to that we would obtain for ϵ_2 at the indirect edge if there was resonance on the intermediate state. Therefore, we compare: $\epsilon_{2 \text{ direct}} = 30\,000 \text{ cm}^{-1}$ to $K\epsilon_{2 \text{ ind}} = 10K \text{ cm}^{-1}$. The correction factor K , takes account of the fact that we must include the resonance in the energy denominator of $\epsilon_{2 \text{ ind}}$, given by Eq. (1). We put

$$K = \frac{(\delta E - \hbar\omega_p)_{\text{GaP}}^2}{(\delta E' - \hbar\omega_p + \Gamma)_{\text{GaInP}}^2}.$$

The numerator is evaluated for GaP, $\delta E = \Gamma_{1c} - X_{1c} = 500 \text{ meV}$; the denominator represents the energy denominator we must have for the alloy resonance, $\delta E' = \hbar\omega_p$ and $\Gamma = 10 \text{ meV}$ is evaluated from the half-width of our spectra.

This gives $K\epsilon_{2 \text{ ind}} \approx 25\,000 \text{ cm}^{-1}$ to be compared to $30\,000 \text{ cm}^{-1}$ for $\epsilon_{2 \text{ direct}}$. This elementary calculation shows that, at the resonance of the indirect gap, the contribution to ϵ_2 is of the same order of magnitude as that of a direct gap, and so are the discontinuities in ϵ_1 .

We have to note that the expression used for ϵ_2

[Eq. (1)] is obtained from integration on the density of states, keeping the denominator constant. So, this expression gives a poor approximation at energies near the resonance. More careful calculation of $\epsilon_{2 \text{ ind}}$, keeping the energy denominator under the integral, shows³⁶ that near the resonance $\epsilon_{2 \text{ ind}}$ has a square-root energy dependence which gives a threshold comparable to the direct one.

This explains why, near the crossover of the Γ and L conduction minima, we observe a drastic modification of $\Delta R/R$, i.e., of $\Delta\epsilon_1$. The resulting line shape of Fig. 16 is easily understood, combining two similar structures [Fig. 11(b)] at energies slightly different.

This resonance has also been observed at lower temperature on a sample with lower gallium content ($x = 0.69$). Figure 18 gives the $\Delta R/R$ spectra obtained at 10°K , which shows the proximity of the direct and indirect edges. In Figs. 19 and 20 we show from the preceding discussion, that this time, the Γ - L crossover occurs around 70 – 100°K , in agreement with the expected evolution of the transition energies with composition.

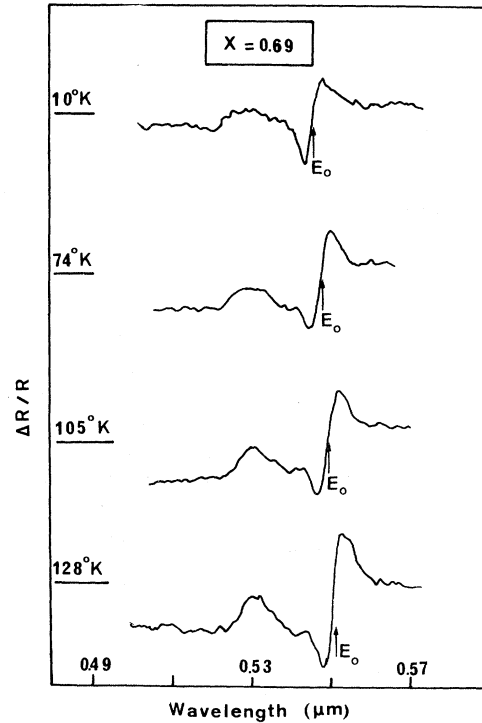


FIG. 19. Temperature evolution of the $\Delta R/R$ spectra obtained on $\text{Ga}_{0.69}\text{In}_{0.31}\text{P}$ sample. The extra oscillation characteristic of resonant indirect transitions occurs, here, at lower temperature than for $x = 0.72$ sample.

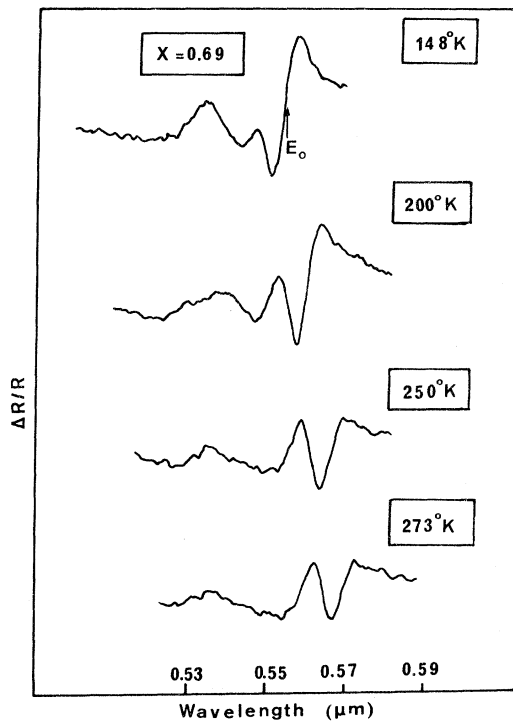


FIG. 20. Same as Fig. 19.

D. $L - X$ crossover

The preceding results show that at low temperature, for composition $x > 0.84$, the fundamental edge is indirect and involves the X_{1c} minima of the conduction band, while for $0.68 < x < 0.72$ the edge remains indirect but involves the L_{1c} minima. Thus, we may expect to observe an $X - L$ crossover for $\text{Ga}_x\text{In}_{1-x}\text{P}$ samples of intermediate composition.

This, has been observed at 10°K on a sample of composition $x = 0.77$. This result is illustrated in Fig. 21. Taking account of the phase inversion of the structures, due to the different modulation of the X and L minima, near the $X - L$ crossover we may observe a mixing of positive and negative structures with an $E^{-1/2}$ energy dependence, corresponding to the different indirect absorption processes assisted by the $\text{LA}(X)$ and $\text{LO}(L)$ or $\text{LA}(L)$ phonons.

That is what we observed in Fig. 21. At 10°K we obtain $E_{\text{ind}}(L) - E_{\text{ex}} + \hbar\omega_{\text{LO}}(L) = 2.329 \text{ eV}$ and $E_{\text{ind}}(X) - E_{\text{ex}} + \hbar\omega_{\text{LA}}(X)$ at a slightly higher energy. The mixing of the structures does not permit us to determine accurately the energy at which it occurs. We must note that at higher temperature the increase of absorbed phonons increases the main absorption and screens the high-energy structure. From the line shape of Figs. 10 and 11

we assign the negative peak to an indirect transition ending at the L minimum, and the positive one to that leading to X minimum.

E. Conclusion: Conduction-band structure of $\text{Ga}_x\text{In}_{1-x}\text{P}$ alloys

All the preceding results are summarized in Fig. 22, which represents the composition dependence of the energy of the direct and indirect gaps at 10°K . The energies of the E_0 gaps are obtained, on samples with rough back faces, from the energy at which the inflexion point of structures similar to those shown in Figs. 23–25 occurs. The energies of the indirect edges, plotted in Fig. 22 correspond to $E_{\text{ind}} - E_{\text{ex}} + \hbar\omega_{\text{LA}}(X)$ for the X minima and to $E_{\text{ind}} - E_{\text{ex}} + \hbar\omega_{\text{LO}}(L)$ for the L minima. We used these energies because they are the most accurate we can deduce from the main scattering processes we have observed in differential spectroscopy.

Extrapolating these values to those given by Onton *et al.*³⁷ for the energy position of X minima, and by White *et al.*³⁸ for the direct gap value of

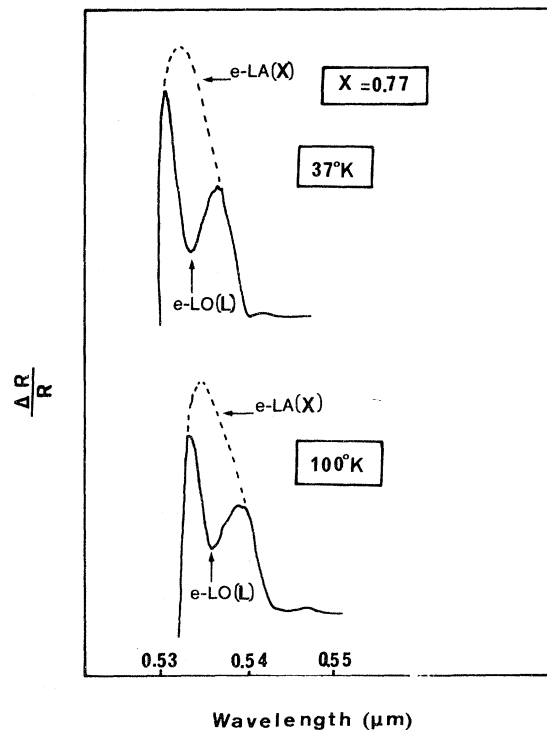


FIG. 21. $\Delta T/T$ spectra obtained on $x = 0.77$ sample at different temperatures. As discussed in the text, structures characteristic of L and X , indirect transitions (dashed line for X) are superimposed out of phase. The assignment to the conduction band minima is obtained from the phase relation we can deduce from the structures of Fig. 10.

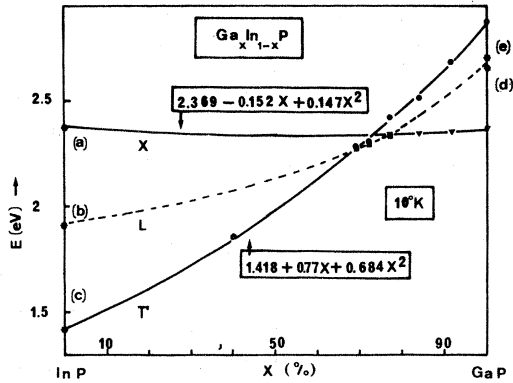


FIG. 22 Composition dependence of the direct (●) and indirect (▼;Γ-X and ■:Γ-L) gaps. For the indirect edges the energy values correspond to $(E_{ind X} - E_{ex} + \hbar\omega_{LA}(X))$ and $(E_{ind L} - E_{ex} + \hbar\omega_{LO}(L))$ which are the energies of the more accurate structures we can obtain in differential spectroscopy. Solid stars correspond to the values obtained from (a) Ref. 10; (b) Ref. 12; (c) Ref. 13; (d) Ref. 14; (e) Ref. 15.

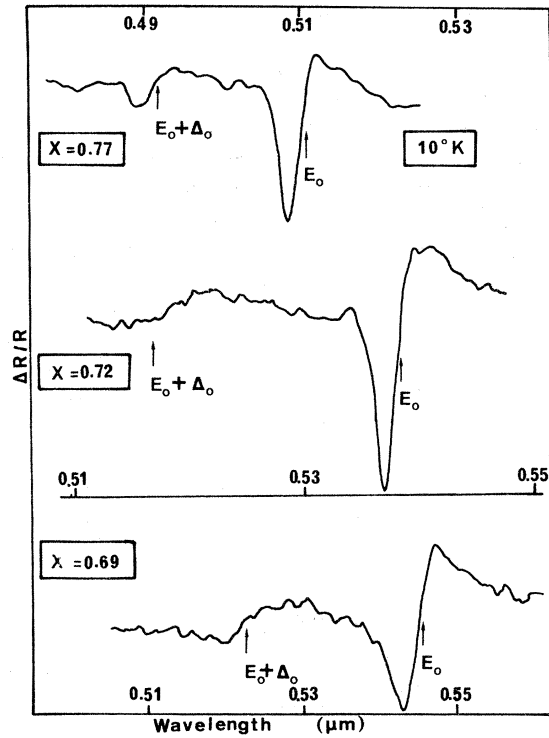


FIG. 24. Same as Fig. 23.

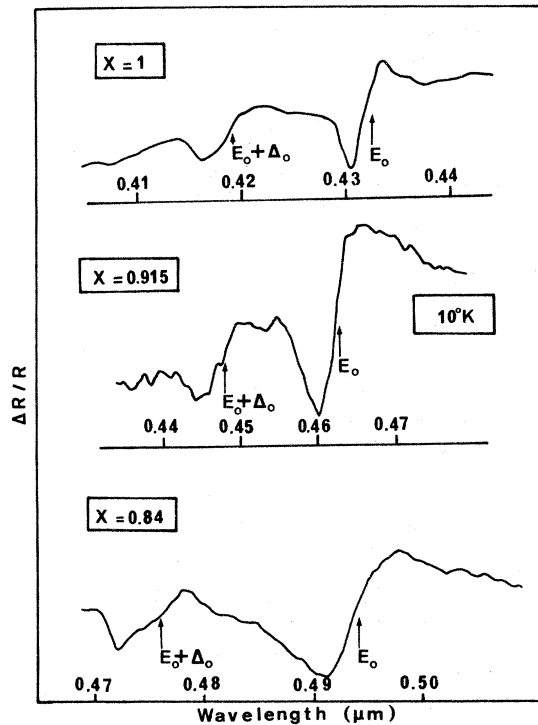


FIG. 23. Piezoreflection spectra in the range of E_0 and $E_0 + \Delta_0$ gaps for composition values: $x=1, 0.915, 0.84, 0.77, 0.72, 0.69,$ and 0.39 .

InP, we can represent the x dependence of the direct and X indirect gaps of $Ga_xIn_{1-x}P$ by the equations

$$E_{direct}(x) = 1.418 + 0.77x + 0.684x^2,$$

$$E_{X\ ind}(x) = 2.369 - 0.152x + 0.147x^2.$$

For composition values greater than $x=0.80$ it has not been possible to observe on very thin samples, sharp structures characteristic of the L minima. The energy position of this minima on

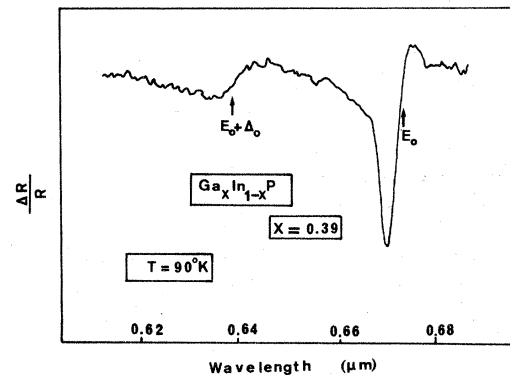


FIG. 25. Same as Fig. 23.

GaP, has been the object of some controversy,^{34,39} so taking account of our results and that of James *et al.*⁴⁰ we just indicate in Fig. 22 the composition dependence we must expect to observe for the energy value of L minima.

In Table II, we collected characteristic energy values obtained in this experiment. We give also, for completeness, some values of the energy and temperature coefficient of E_1 transition we have obtained.

The predicted band-structure variation across the alloy, shown in Fig. 22 permits us to conclude that at 10 °K, the $X_{1c}-L_{1c}$ crossover occurs near $x=0.77$ and that the L_{1c} minima cut Γ_{1c} around $x=0.68$. Using a constant value of 13 meV for the exciton binding energy at X and L ,²⁰ and extrapolating LA(X) and LO(L) phonon energies from pure compound values²⁶ we can deduce from Fig. 23 the $E_{\text{ind } X}-E_{\text{ind } L}$ and $E_0-E_{\text{ind } L}$ crossover values. We obtain

$$x_{X_{1c}-L_{1c}}=0.78 \quad \text{and} \quad x_{\Gamma_{1c}-L_{1c}}=0.65$$

in good agreement with the values deduced by Pitt *et al.*¹⁰ from high-pressure Hall-effect measurements ($x=0.74$ and $x=0.63$, respectively).

In conclusion, the possibility offered by piezomodulation experiments to determine without ambiguity the phase of the structures characteristic of direct and indirect transitions, allows us to separate the contribution of L and X minima to the imaginary part of the dielectric constant. For the first time, we have obtained clear evidence of resonant indirect transitions as would be expected at energies where direct and indirect transitions are superimposed. The values we give for $L-X$ and $\Gamma-L$ crossovers provide a means of reconciling the inconsistencies in interpretation of previous measurements on $\text{Ga}_x\text{In}_{1-x}\text{P}$ alloys.

ACKNOWLEDGMENT

We are grateful to Professor K. C. Rustagi for critical reading this manuscript.

*Centre associé au CNRS.

- ¹For a recent review, see A. Onton, *Festkoerperprobleme*, edited by H. J. Quisser (Vieweg, Braunschweig, 1973), Vol. 13.
- ²A. Onton and R. J. Chicotka, *J. Appl. Phys.* **41**, 4205 (1970).
- ³H. M. Macksey, H. Holonyak Jr., R. D. Dupuis, J. C. Campbell, and G. W. Zack, *J. Appl. Phys.* **44**, 1333 (1973).
- ⁴R. Z. Bachrach and B. W. Hakki, *J. Appl. Phys.* **42**, 5101 (1971).
- ⁵A. Laugier, C. Alibert, and J. Chevallier, *J. Phys. (Paris) Suppl.* **4**, **35**, C 3-77 (1974).
- ⁶A. H. Lettington, D. Jones, and R. Sarginson, *J. Phys. C* **4**, 1534 (1971).
- ⁷Zh. I. Alferov, D. Z. Garbuzov, S. G. Konnikov, P. S. Kop'ev, V. A. Mishurnyi, V. D. Rumyantsev, and D. N. Tret'yakov, *Sov. Phys.-Semicond.* **7**, No. 3, 435 (1973).
- ⁸A. Onton and M. R. Lorentz, in *Proceedings of the Tenth International Conference on the Physics of Semiconductors*, 1970, Cambridge (unpublished), p. 440.
- ⁹A. Onton, M. R. Lorentz, and W. Reuter, *J. Appl. Phys.* **43**, 3420 (1971).
- ¹⁰G. D. Pitt, M. K. R. Vyas, and A. W. Mabbitt, *Solid State Commun.* **14**, 621 (1974).
- ¹¹D. L. Campausen, G. A. N. Connell, and W. Paul, *Phys. Rev. Lett.* **26**, 184 (1971).
- ¹²H. Mathieu, D. Auvergne, and P. Merle, *Phys. Status Solidi B* **72**, 609 (1975); *Solid State Commun.* **18**, 589 (1976).
- ¹³A. Laugier and J. Chevallier, *Phys. Status Solidi* **7**, 427 (1971).
- ¹⁴R. J. Elliott, *Phys. Rev.* **108**, 1374 (1957).
- ¹⁵I. Balslev, *J. Phys. Soc. Jpn.* **21**, 101 (1966).
- ¹⁶Zallen and W. Paul, *Phys. Rev.* **134**, A1628 (1964).
- ¹⁷A. Gavini and M. Cardona, *Phys. Rev. B* **1**, 672 (1970).
- ¹⁸F. Pollak, C. W. Higginbotham, and M. Cardona, in *Ref. 15*, p. 20.
- ¹⁹F. Gallissot, and R. Vergne, *Publication Scientifique du Ministère de l'Air-France*, **412**, 50 (1965).
- ²⁰D. Auvergne, P. Merle, and H. Mathieu, *Phys. Rev. B* **12**, 1371 (1975).
- ²¹J. L. Birman, M. Lax, and R. Loudon, *Phys. Rev.* **145**, 620 (1966).
- ²²H. Montgomery, *Proc. R. Soc. A* **309**, 521 (1969).
- ²³J. Chevallier, *J. Phys. (Paris) Suppl.* **4**, **35**, C 3-77 (1974).
- ²⁴M. L. Cohen and T. K. Bergtresser, *Phys. Rev.* **141**, 789 (1966).
- ²⁵J. Camassel and D. Auvergne, *Phys. Rev. B* **12**, 3258 (1975).
- ²⁶G. F. Alfrey and P. H. Borchers, *J. Phys. C* **5**, L275 (1972).
- ²⁷I. F. Chang and S. S. Mitra, *Phys. Rev.* **172**, 924 (1968).
- ²⁸R. Beserman, C. Hirleman, M. Balkanski, and J. Chevallier, *Proceedings of the Third Conference on Light Scattering in Solids, Campinas, Brazil, 1975*, edited by M. Balkanski (Pergamon, London, 1975).
- ²⁹A. Onton and L. M. Foster, *J. Appl. Phys.* **43**, 5084 (1972).
- ³⁰G. Lucovsky, M. H. Brodsky, M. F. Chen, R. J. Chicotka, and A. T. Ward, *Phys. Rev. B* **4**, 1945 (1971).
- ³¹B. O. Seraphin and N. Bottka, *Phys. Rev.* **145**, 628 (1966).
- ³²H. Mathieu, J. Camassel, and D. Auvergne, *Phys. Status Solidi B* **68**, 797 (1975).
- ³³M. Cardona, *Solid State Physics*, Suppl. 11 (Academic, New York, 1969).
- ³⁴W. P. Dumke, M. R. Lorentz, and G. D. Pettit, *Phys. Rev. B* **5**, 2978 (1972).
- ³⁵P. J. Dean, G. Kaminsky, and R. B. Zetterstrom, *J. Appl. Phys.* **38**, 3551 (1967).
- ³⁶W. P. Dumke, M. R. Lorentz, and G. D. Pettit, *Phys. Rev. B* **5**, 2978 (1972).

³⁷A. Onton, R. J. Chicotka, and Y. Yacoby, in *Proceedings of the Eleventh International Conference of the Physics of Semiconductors* (Polish Scientific, Warsaw, 1972).

³⁸A. M. White, P. J. Dean, L. L. Taylor, R. C. Clarke,

D. J. Ashen, and J. B. Mullin, *J. Phys. C* 5, 1727 (1972).

³⁹P. J. Dean, G. Kaminsky, and R. B. Zetterstrom, *J. Appl. Phys.* 38, 3551 (1967).

⁴⁰L. W. James, J. P. Van Dyke, F. Herman, and D. M. Chang, *Phys. Rev. B* 1, 3998 (1970).